Vorticity alignment of rigid fibers in an oscillatory shear flow: Role of confinement

Braden Snook, Elisabeth Guazzelli, Jason E. Butler

Vorticity alignment of rigid fibers in an oscillatory shear flow: Role of confinement

Braden Snook, Elisabeth Guazzelli, and Jason E. Butler

Citation: Phys. Fluids **24**, 121702 (2012); doi: 10.1063/1.4770141
View online: http://dx.doi.org/10.1063/1.4770141
View Table of Contents: http://pof.aip.org/resource/1/PHFLE6/v24/i12
Published by the American Institute of Physics.

PHYSICS OF FLUIDS **24**, 121702 (2012)

Vorticity alignment of rigid fibers in an oscillatory shear flow: Role of confinement

Braden Snook,[1] Elisabeth Guazzelli,[2] and Jason E. Butler[1]
[1]*Department of Chemical Engineering, University of Florida, Gainesville, Florida 32611, USA*
[2]*Aix-Marseille Université, CNRS, IUSTI UMR 7343, 13453 Marseille Cedex 13, France*

(Received 9 October 2012; accepted 23 November 2012; published online 11 December 2012)

Rigid fibers suspended in a viscous, Newtonian fluid at high concentrations can be aligned in the direction perpendicular to the flow-gradient plane (vorticity direction) by applying an oscillatory shear flow. A simple model, which considers only excluded volume and self-mobilities, can accurately predict the orientation distributions measured in experiments by Franceschini *et al.* ["Transverse alignment of fibers in a periodically sheared suspension: An absorbing phase transition with a slowly varying control parameter," Phys. Rev. Lett. **107**, 250603 (2011)]. Furthermore, simulations reveal that the alignment of the fibers in the vorticity direction depends strongly on the presence of the bounding walls. © *2012 American Institute of Physics*. [http://dx.doi.org/10.1063/1.4770141]

The rheological and mechanical properties of suspensions composed of rod-like particles are sensitive to the spatial and orientational distribution of the particles within the suspension. Understanding and controlling the flow-induced alignment of these elongated particles is of fundamental importance and has implications for numerous material processing applications, such as the manufacture of paper[1] and fiber composites.[2]

Recent measurements[3] indicated that the orientation distribution in semi-concentrated suspensions of non-colloidal fibers can be controlled by altering the strain amplitude within an oscillatory shear flow. The orientation distribution changes little from the initial state at sufficiently small amplitudes of strain. At large strain amplitudes, the fibers align in the direction of the flow, similarly to the steady shearing flow of a suspension of rigid fibers.[4,5] While these results might be expected, the experiments also measured a strongly preferred alignment of the fibers in the vorticity (transverse to both the flow and gradient planes) direction for intermediate strain amplitudes. This surprising result remains to be understood. Alignment with the vorticity direction is observed when oscillating fibers suspended in a weakly elastic fluid.[6] However, the experiments[3] of interest here were performed with a Newtonian fluid. For an elastic fluid, the orientation of even a single fiber spins toward the vorticity direction,[7,8] whereas the orientation of a single fiber oscillated in a Newtonian fluid traces a reversible path defined by the Jeffery orbit corresponding to the initial orientation.[9]

The irreversible dynamics of suspensions of non-colloidal particles suspended and sheared in Newtonian fluids has been studied extensively; the vast majority of work has focused on spherical particles, but early work used fibers.[9–11] The reversibility of the Stokes equations implies that the particles should retrace their paths upon reversal of the flow. However, any small source of irreversibility in a physical system (e.g., Brownian motion, particle surface roughness, particle deformability, or inertia) causes a loss of memory. Oscillating the suspensions provides a particularly convenient format for studying irreversibility in suspension systems.[12,13] For sufficiently large strains and concentrations, particles do not return to their starting configurations after one or more cycles and their displacements exhibit a chaotic, random motion. The need for relatively large concentrations of particles implies that short-range interactions are the primary origin of the chaotic behavior.

This work addresses the origin of the unexpected and irreversible alignment of the fibers in the direction of vorticity, which cannot be attributed to the elasticity of the suspending fluid.

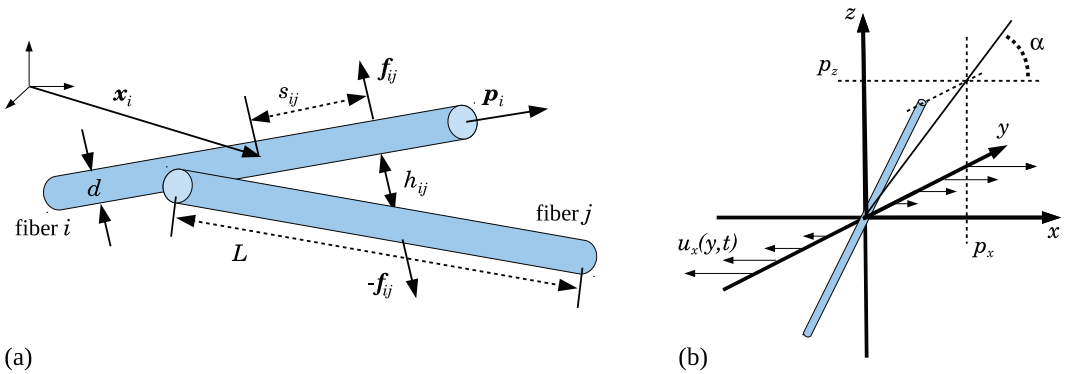

FIG. 1. (a) Each fiber of aspect ratio $A = L/d$ is described by its center of mass $\boldsymbol{x}_i$ and orientation $\boldsymbol{p}_i$. A repulsive force acts between two fibers i and j at the points of closest approach separated by the distance h_{ij}. (b) The x-direction is that of the flow; the flow varies linearly in the y-direction, or gradient direction, and the vorticity axis is in the z-direction. The fiber's projection on the flow-vorticity plane and the flow direction forms the angle α: $\cos^2(\alpha) = p_x^2/(p_x^2 + p_z^2)$.

Rather the vorticity alignment, and other behaviors of the orientation distribution, was attributed by Franceschini *et al.*[3] to short-range interactions between fibers in a process that can drive the system into a reversible, or "absorbing," state. A simple algorithm demonstrates that short-range interactions between particles can account for alignment in the vorticity direction, depending upon the concentration and strain amplitude. The model reveals that the extent of alignment depends strongly on whether or not the suspension of fibers is confined in the gradient direction by closely-spaced bounding walls. Only those simulations with a wall-spacing matching that used in the experiments accurately predict the mean orientation reported by Franceschini *et al.*[3]

The model is similar to that used by Sundararajakumar and Koch[5] to simulate the steady shear of semi-concentrated suspensions of rigid fibers. The motion of each fiber is determined by a balance between the hydrodynamic drag forces and short-range forces used to maintain the excluded volume. Inertia is ignored in these calculations, since both the maximum Reynolds number and frequency of oscillation were small in the experiments. Long range fluid disturbances, or hydrodynamic interactions, are neglected within the model, as they have little impact on dynamics in the semi-concentrated regime;[5] comparing results of steady shear from this model with simulations with hydrodynamic interactions[14] confirms the assertion.

The motion of each rigid fiber, i, is fully described by the center-of-mass velocity, $\dot{\boldsymbol{x}}_i$, and the rotational velocity, $\dot{\boldsymbol{p}}_i$, where $\boldsymbol{x}_i$ and $\boldsymbol{p}_i$ are the center-of-mass position and unit vector parallel to the fiber's major axis as shown in Fig. 1. The center-of-mass motion is

$$\dot{\boldsymbol{x}}_i = \boldsymbol{u}(\boldsymbol{x}_i) + \xi^{-1}\left(\boldsymbol{I} + \boldsymbol{p}_i\boldsymbol{p}_i\right)\cdot\boldsymbol{F}_i \tag{1}$$

and rotational motion is

$$\dot{\boldsymbol{p}}_i = \boldsymbol{\Omega}\cdot\boldsymbol{p}_i + B\left(\boldsymbol{I} - \boldsymbol{p}_i\boldsymbol{p}_i\right)\cdot\boldsymbol{E}\cdot\boldsymbol{p}_i + \frac{12\xi^{-1}}{L^2}\boldsymbol{\mathcal{T}}_i\times\boldsymbol{p}_i. \tag{2}$$

The mobility of the center-of-mass is $\xi^{-1}\left(\boldsymbol{I} + \boldsymbol{p}_i\boldsymbol{p}_i\right)$, where $\xi^{-1} = \ln(2A)/4\pi\mu L$, μ is the fluid viscosity, L is the fiber length, $A = L/d$ is the aspect ratio, and d is the fiber diameter. The mobility is derived from slender-body theory.[15,16] A simple oscillatory shear, $\boldsymbol{u}(\boldsymbol{x},t) = \dot{\gamma}(t)\,y\boldsymbol{e}_x$, is imposed, with flow in the $x-$direction and the gradient in the $y-$direction as shown in Fig. 1. The shear rate, $\dot{\gamma}(t)$, is a square wave of magnitude one and the period is determined by the strain amplitude, γ.

In the absence of collisions, each fiber translates with the velocity evaluated at the center-of-mass, $\boldsymbol{u}(\boldsymbol{x}_i)$, and rotates in a Jeffery orbit:[17] the orientation rotates fully with the rate of rotation of the flow, $\boldsymbol{\Omega} = \frac{1}{2}\left[(\nabla\boldsymbol{u}) - (\nabla\boldsymbol{u})^T\right]$, and only a fraction $B = \left(A_e^2 - 1\right)/\left(A_e^2 + 1\right)$ of the rate of extension of the flow, $\boldsymbol{E} = \frac{1}{2}\left[(\nabla\boldsymbol{u}) + (\nabla\boldsymbol{u})^T\right]$. The aspect ratio A has been replaced by an effective one, A_e, in the parameter B. The effective ratio, as developed through experiment and theory,[18–20] accounts for the rotation of a spherocylinder as opposed to an ellipsoidal particle, for which Jeffery[17] originally derived the equation.

Collisions between the fibers alter the motion of both the center-of-mass and orientation. To prevent the overlap of a fiber i with a fiber j, a short range repulsive force is applied,

$$\boldsymbol{f}_{ij} = \begin{cases} 0 & \text{if } h_{ij} > \epsilon, \\ f_0 \boldsymbol{n}_{ij} & \text{if } h_{ij} \leq \epsilon, \end{cases} \tag{3}$$

where h_{ij} is the minimum separation distance between two fibers and $\boldsymbol{n}_{ij}$ is their common normal, $\pm\left(\boldsymbol{p}_i \times \boldsymbol{p}_j\right) / \left|\boldsymbol{p}_i \times \boldsymbol{p}_j\right|$. The sign of the normal is chosen so that the force repels the fibers and the force on fiber j is equal and opposite to that on i, hence there is no net force. The simulation results are insensitive to the exact form of the repulsive force used, so long as the range is small compared to the fiber diameter and the displacements caused by the force are resolved at a fine level by holding the time step small. Here, the range ϵ is set to $0.1d$ and the force $f_o = |\dot{\gamma} L \xi / 2|$. On rare occasions when fibers overlap, the force f_o is increased relative to the overlap distance, ensuring that the particles separate.

All interactions on fiber i sum to give the total, non-hydrodynamic force $\boldsymbol{F}_i$,

$$\boldsymbol{F}_i = \sum_{j=1}^{N_f} \boldsymbol{f}_{ij}, \tag{4}$$

and torque $\boldsymbol{\mathcal{T}}_i$,

$$\boldsymbol{\mathcal{T}}_i = \sum_{j=1}^{N_f} s_{ij} \boldsymbol{p}_i \times \boldsymbol{f}_{ij}, \tag{5}$$

where s_{ij} is the point along fiber i at which the collision occurs with fiber j and the sums exclude the occurrences of $i = j$. The total number of fibers simulated, N_f, is set by the concentration and size of the simulation box.

The concentration of fibers and strain amplitude are varied within the simulations. The aspect ratio is set to $A = 11$ to correspond with the experiments and $A_e = 8.8$. For fully periodic calculations that utilize Lee-Edward's boundary conditions, the simulation box is cubic with a length of $3.25L$. For simulations with boundaries, fibers are confined in the gradient direction by applying the same force between a fiber and the wall as used between contacting fibers. The wall separation of $1.45L$ used in the simulations corresponds to that used in the experiments of Franceschini *et al.*[3] Periodic boundaries in the flow and vorticity directions are separated by $5.25L$. The number of particles simulated ranges from 265 to 1232, corresponding to volume fractions ϕ of 0.05 to 0.20. Equations (1) and (2) are integrated using an Euler method with an adaptive time step selected to maintain a maximum displacement less than $0.01d$. Twelve initial configurations were used to calculate each mean value and reported errors are those between the mean values of each configuration.

Primarily, two measures are calculated from the data generated by the simulations and presented here: one for the average orientations and another that tracks the irreversible activity of the suspension of fibers. The order parameter $S_\alpha = 1 - 2\langle \cos^2(\alpha) \rangle$ is calculated from the simulation results to facilitate comparison with the experimental measurements[3] of alignment that were reported solely in terms of this parameter. As shown in Fig. 1, the angle α is that between the flow direction (x) and the projection of a fiber's orientation onto the flow-vorticity (x-z) plane; the brackets, $\langle \cdot \rangle$, indicate an average over all runs and fibers. Note that S_α is 0 for a suspension having a random orientation distribution and is either -1 or 1 for a suspension of fibers aligned perfectly with the flow or vorticity direction, respectively. The number of contacts between fibers are counted over each oscillation and reported as N_c. In this model, irreversible motions of the particles are generated only by contact forces, thus, N_c is a measure of irreversible activity within the suspension.

Figure 2(a) compares experimentally measured and calculated values of S_α as a function of strain amplitude. Simulations with boundaries separated by a distance equivalent to the experiments captures the trend of the alignment behavior, including the surprising alignment of the fibers with the vorticity direction in the vicinity of $\gamma \approx 3$. Using fully periodic boundaries does not reproduce the experimental results. Figure 2(b) visualizes the orientation distribution changes with the number of oscillations, N, for a simulation at $\gamma = 3$ with confining walls. The orientation is random for

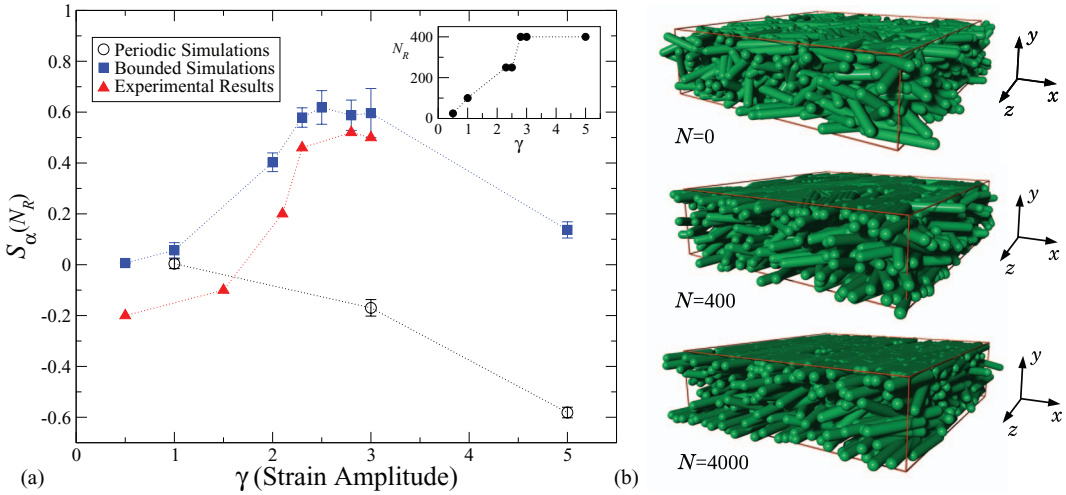

FIG. 2. (a) Comparison of simulation results for S_α with the experimental values for $\phi = 0.20$ and at the the last oscillation reported by Franceschini *et al.*[3] The inset shows the oscillation number (N_R) at which the data were reported. (b) Images of the microstructure from a simulation with boundaries, $\phi = 0.20$, and $\gamma = 3$ prior to oscillating ($N = 0$), at the last point recorded in the experiments ($N = 400$), and at steady state ($N = 4000$) (enhanced online) [URL: http://dx.doi.org/10.1063/1.4770141.1] [URL: http://dx.doi.org/10.1063/1.4770141.2] [URL: http://dx.doi.org/10.1063/1.4770141.3].

the initial condition at $N = 0$ and progressively aligns in the vorticity direction through $N = 400$, corresponding to the point at which the comparison is made with experiments in Fig. 2(a). The simulation predicts an increasing alignment of the fibers with the vorticity direction until reaching a steady state at $N \approx 4000$. Figure 3(a) provides more details about the evolution of S_α with N and shows that the value of S_α for $\gamma = 3$ transitions from 0.60 at $N = 400$ to 0.70 at $N = 4000$; the significant difference in the orientation distribution represented by this difference of 0.1 in the value of S_α is demonstrated in Fig. 2(b).

Figure 3(a) shows that significant changes in orientation occur when oscillating with $\gamma > 1$. The curves exhibit an initial decrease in S_α, indicating a movement toward flow alignment for initial oscillations, followed by an increase that is more pronounced for simulations with boundaries. In this latter case, S_α attains positive values that reflect a vorticity alignment of the fibers. Note that the initial distribution, both spatial and orientational, is a random one in the simulations, whereas steady shear was applied in the experiments before beginning the oscillations. This may explain the lack of an initial decrease in S_α as reported in the third figure of Franceschini *et al.*[3]

Figure 3(b) shows that an order of magnitude reduction in the number of collisions between fibers occurs for $\gamma = 3$ and 5 for simulations with bounding walls. A similar trend is observed for simulations without confinement for the same strain amplitudes, though N_c is an order of magnitude larger. In these cases, N_c reaches steady state by the same value of N as S_α. The number of collisions also decreases with N for $\gamma = 1$, but a steady state is not obtained within the same number of cycles as S_α. Though S_α does not change significantly, individual fibers continue to change orientation due to contacts.

Franceschini *et al.*[3] interpreted the lack of a change in the order parameter S_α after the first few oscillations for $\gamma < 2.2$ to the suspension attaining an absorbing state in which individual particles return to their starting positions and orientations after each cycle. They also associated the vorticity alignment with the attainment of an absorbing state, whereas Fig. 3 indicates activity across all strain amplitudes for the duration of the simulations. The discrepancy between the numerical predictions and experimental measurements of activity could be explained by resolution limits in the measurements. The simulations predict orientation changes and displacements of only a few microns for individual particles at $\gamma = 1$ and $N > 10$; such small changes would be difficult to detect even with a microscope. Also, lubrication interactions that exist between fibers in the viscous fluid could prevent, or at least reduce, the occurrence of contacts. The question of the existence of contacts in the presence of lubricating fluids is a question of active investigation for suspensions of spheres,[21,22]

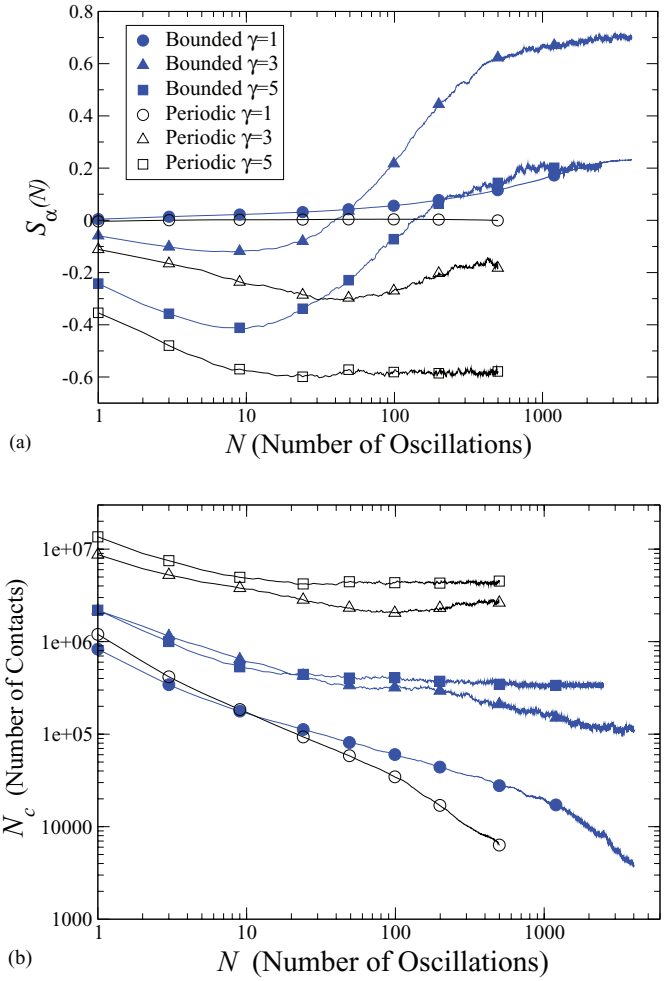

FIG. 3. Results for a volume fraction of $\phi = 0.20$. (a) The evolution of S_α with the number of oscillations for both the periodic and bounded simulations. (b) The total number of collisions, N_c, experienced between the fibers during each oscillation.

though arguments[23] that contacts are more likely between fibers than spheres have been made. The current simulations do not include lubrication with the goal of generating a minimal model that can explain the unexpected alignment phenomena.

All data presented up to this point have been for a volume fraction of 0.20. Figure 4 shows the steady values of S_α at $\phi = 0.20$ and two additional volume fractions. At the lower volume fraction of 0.05, the orientation of the fibers tend to align more with the flow, rather than the vorticity, direction for both the bounded and unbounded cases.

Confining the fibers has the most impact on the orientation distribution at $\phi = 0.20$ and $\gamma = 3$, where the results of simulations with full periodicity predict a mean alignment in the direction of flow. The probability distribution of the angle α given in Fig. 5(a) shows the small preference for flow alignment when using periodic boundaries and also quantifies, with more detail, the strong alignment in the vorticity direction when using bounding surfaces.

The maximum extent of alignment is predicted at $\phi = 0.15$ and $\gamma = 3$, where $S_\alpha = 0.88 \pm 0.02$ for the simulations of confined fibers. Using fully periodic boundaries for the same concentration and strain amplitude also generates a preferred alignment in the vorticity direction, where $S_\alpha = 0.60 \pm 0.05$. Comparing the details of the distributions, as done in Fig. 5(b), demonstrates the significant orientation difference between the two types of boundary conditions.

This latter result shows that bounding walls are not required to achieve some alignment of the fibers in the vorticity direction, but confining the fibers clearly enhances the extent of organization

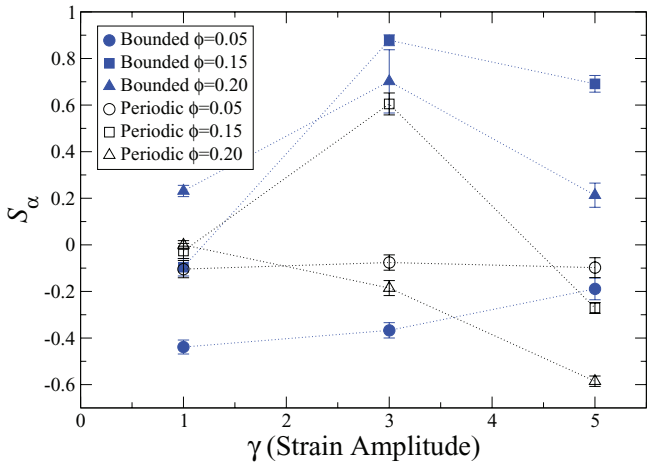

FIG. 4. Steady values of the order parameter S_α as a function of strain amplitude for simulations performed with fully periodic boundaries (Periodic) and with bounding walls (Bounded).

and alignment in the vorticity direction. The alignment phenomena, whether in the flow or vorticity direction, are a complex function of the interactions between the imposed straining flows and their amplitude, the concentration of the fibers, and the geometry of the shear cell.

Confining elongated particles between bounding walls generally promotes organization of the orientations, as for liquid crystals, which transition from an isotropic to nematic phase when squeezed between planar walls.[24] Likewise, the boundaries impose some order on the particles in the immediate vicinity of the wall (see Fig. 2(b)), even for the initial condition; fluctuations in orientation generated by the oscillatory shear, rather than thermal fluctuations as for liquid crystals, provide the mechanism for the particles to search for a favorable arrangement. Perhaps, the more interesting point here is the preference for vorticity, versus flow, alignment.

The lack of a boundary that organizes the orientations results in a significantly lower extent of, or even no, alignment in the direction of vorticity as compared to the bounded simulations. A simple test was performed to verify that the solid boundaries themselves, and neither the initial orientation distribution created by the walls, nor different geometry of the simulation box, are responsible for the vorticity alignment predicted by the simulations. The initial distributions were generated within the bounded cell, but then the simulation was performed with periodic boundaries. These simulations returned only a slightly lower tendency for the fibers to align in the flow direction. For $\phi = 0.20$ and $\gamma = 3$, the simulation predicts $S_\alpha = -0.08 \pm 0.03$ at $N = 400$, which is close to the value of $S_\alpha = -0.17 \pm 0.03$ for periodic boundaries when starting from a random particle configuration.

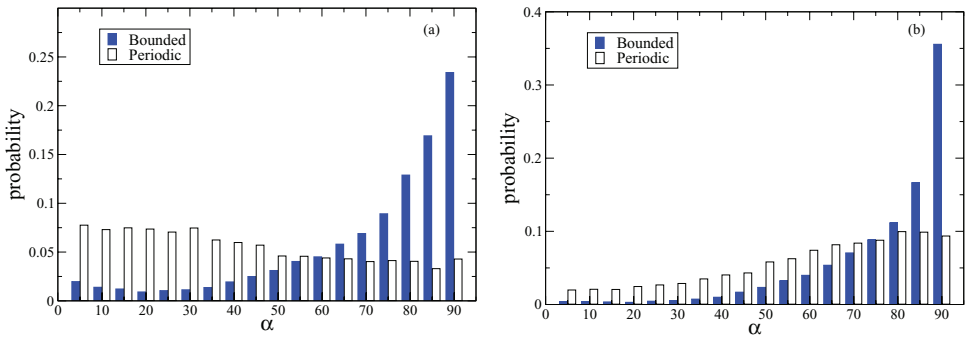

FIG. 5. The probability distribution of the angle α, where 0^o is the flow direction and 90^o is the vorticity direction (see Fig. 1), at steady state for bounded and fully periodic conditions. Results for a volume fraction of (a) $\phi = 0.20$ and (b) $\phi = 0.15$. Note that the plots utilize different scales.

The sensitivity of the fiber alignment on the initial distribution was explored further by aligning the suspension in steady shear prior to oscillating, as was done in the experiments.[3] For $\phi = 20$ with $\gamma = 3$ and bounding walls, the simulations with the pre-shear predict that any differences in the mean alignment disappear by $N = 400$, where the pre-sheared cases give $S_\alpha = 0.63 \pm 0.05$ and the initially random, but confined, distributions give $S_\alpha = 0.6 \pm 0.1$.

In conclusion, the minimal model employed here, which considers only self-mobilities and excluded volume of the fibers, reproduces the experimental observation[3] of vorticity alignment of the orientation distribution for oscillatory shear when boundaries are included. Franceschini *et al.*[3] attributed the vorticity alignment to particle-particle collisions solely, omitting the wall contributions. Though some alignment can occur without confining the suspension, the confinement clearly plays a strong role in the experimental observations, which utilized a wall spacing of 1.45 fiber lengths. Accordingly, a simple and complete principle of organization is still lacking as the alignment depends subtly upon three factors: the amplitude of the straining flow, the concentration of the fibers, and the boundary conditions. For the latter factor, only the two cases of fully periodic boundaries and a wall separation identical to that in the experiments were considered. The wall separation at which the orientational dynamics of the suspension transitions from the highly confined to the unbounded behavior remains to be explored.

The assistance of Mr. Rusty Stiles with running the simulation code and organizing the results is greatly appreciated. We also thank Dr. Franceschini and Professor Pine for their comments and discussion. This work was supported by the Partner University Fund for particulate flows and the National Science Foundation (Grant No. 0968313).

[1] F. Lundell, L. D. Söderberg, and P. H. Alfredsson, "Fluid mechanics of papermaking," Ann. Rev. Fluid Mech. **43**, 195 (2011).
[2] T. D. Papathanasiou and D. C. Guell, *Flow-Induced Alignment in Composite Materials* (Woodhead, 1997).
[3] A. Franceschini, E. Filippidi, E. Guazzelli, and D. J. Pine, "Transverse alignment of fibers in a periodically sheared suspension: An absorbing phase transition with a slowly varying control parameter," Phys. Rev. Lett. **107**, 250603 (2011).
[4] C. A. Stover, D. L. Koch, and C. Cohen, "Observations of fiber orientation in simple shear flow of semi-dilute suspensions," J. Fluid Mech. **238**, 277 (1992).
[5] R. R. Sundararajakumar and D. L. Koch, "Structure and properties of sheared fiber suspensions with mechanical contacts," J. Non-Newtonian Fluid Mech. **73**, 205 (1997).
[6] M. P. Petrich, M. Chaouche, D. L. Koch, and C. Cohen, "Oscillatory shear alignment of a non-Brownian fiber in a weakly elastic fluid," J. Non-Newtonian Fluid Mech. **91**, 1 (2000).
[7] L. G. Leal, "The slow motion of slender rod-like particles in second-order fluid," J. Fluid Mech. **69**, 305 (1975).
[8] Y. Iso, D. L. Koch, and C. Cohen, "Orientation in simple shear flow of semi-dilute fiber suspensions. 1. Weakly elastic fluids," J. Non-Newtonian Fluid Mech. **62**, 115 (1996).
[9] A. Okagawa, G. J. Ennis, and S. G. Mason, "Memory impairment in flowing suspensions. I. Some theoretical considerations," Can. J. Chem. **56**, 2815 (1978).
[10] A. Okagawa and S. G. Mason, "Suspensions: Fluids with fading memories," Science **181**, 159 (1973).
[11] G. J. Ennis, A. Okagawa, and S. G. Mason, "Memory impairment in flowing suspensions. II. Experimental results," Can. J. Chem. **56**, 2824 (1978).
[12] V. Breedveld, D. van den Ende, R. Jongschaap, M. Bosscher, and J. Mellema, "Measuring shear-induced diffusion and rheology of noncolloidal suspensions: Time scales and particle displacements," J. Chem. Phys. **114**, 5923 (2001).
[13] D. J. Pine, J. P. Gollub, J. F. Brady, and A. M. Leshansky, "Chaos and threshold for irreversibility in sheared suspensions," Nature (London) **438**, 997 (2005).
[14] J. Wu and C. K. Aidun, "A numerical study of the effect of fibre stiffness on the rheology of sheared flexible fibre suspensions," J. Fluid Mech. **662**, 123 (2010).
[15] G. K. Batchelor, "Slender-body theory for particles of arbitrary cross-section in Stokes flow," J. Fluid Mech. **44**, 419 (1970).
[16] R. G. Cox, "The motion of long slender bodies in a viscous fluid. Part 1. General theory," J. Fluid Mech. **44**, 791 (1970).
[17] G. B. Jeffery, "The motion of ellipsoidal particles immersed in a viscous fluid," Proc. R. Soc. London, Ser. A **102**, 161 (1922).
[18] F. P. Bretherton, "The motion of rigid particles in a shear flow at low Reynolds number," J. Fluid Mech. **14**, 284 (1962).
[19] B. J. Trevelyan and S. G. Mason, "Particle motions in sheared suspensions. I. Rotations," J. Colloid Sci. **6**, 354 (1951).
[20] S. G. Mason and R. J. Manley, "Particle motions in sheared suspensions: Orientations and interactions of rigid rods," Proc. R. Soc. London, Ser. A **238**, 117 (1956).
[21] P. A. Arp and S. G. Mason, "The kinetics of flowing dispersions. IX. Doublets of rigid spheres (experimental)," J. Colloid Interface Sci. **61**, 44 (1976).
[22] B. Metzger and J. E. Butler, "Clouds of particles in a periodic shear flow," Phys. Fluids **24**, 021703 (2012).
[23] M. P. Petrich and D. L. Koch, "Interactions between contacting fibers," Phys. Fluids **10**, 2111 (1998).
[24] P. G. de Gennes and J. Prost, *The Physics of Liquid Crystals* (Oxford University Press, Oxford, 1993).